Aerosol fabrication of hollow mesoporous silica nanoparticles and encapsulation of L-methionine as a candidate drug cargo†

Xingmao Jiang,[ab] Timothy L. Ward,[a] Yung-Sung Cheng,[b] Juewen Liu[c] and C. Jeffrey Brinker*[ade]

Received (in Berkeley, CA, USA) 22nd December 2009, Accepted 3rd March 2010
First published as an Advance Article on the web 25th March 2010
DOI: 10.1039/b927025f

Hollow spherical nanoparticles with ordered mesoporous silica shells were fabricated by evaporation-induced self-assembly using $(NH_4)_2SO_4$ and cetyltrimethyl ammonium bromide (CTAB) as templates. The model drug, L-methionine, was encapsulated within the spherical void at high loadings by repeated crystallization.

Targeted delivery and sustained release of administered pharmaceutical agents demand a safe, stable, and efficient drug delivery system.[1] Currently, viral vectors, organic cationic compounds, and polymeric and inorganic nanoparticles have been studied as delivery vehicles.[2] Among them, mesoporous silica particles are promising controlled release materials for treatment of various diseases due to their low cost, low toxicity, good biocompatibility, large surface areas, uniform tunable pore sizes, and rich functionality and surface chemistry for imparting molecular recognition and targeted delivery characteristics.[3] Evaporation-induced self-assembly (EISA) has been shown to be a versatile synthetic approach for synthesis of spherical mesoporous silica nanoparticles.[4–7] Corrosion inhibitors and NaCl have been encapsulated into mesoporous silica by EISA, and release can be controlled precisely by pore size, light-responsive valves, and pore surface chemistry.[5] However, developing facile fabrication methods for hollow delivery vehicles exhibiting high drug capacities combined with ordered nanoporous structures for desired release kinetics remains a challenging engineering problem. So far, $CaCO_3$[8] and polystyrene beads[9] have been used to generate hollow silica spheres. The sacrificial templates need to be removed by acid dissolution or high temperature calcination to generate the desired voids in the final silica particles. Phenolic resin has been used to obtain mesoporous carbon/silica and silicon carbide hollow spheres by an aerosol spraying process.[6] Poly(acrylic acid) (PAA) has been encapsulated to prepare hierarchically structured silica particles by EISA.[7] Usually high PAA mass loading results in a population of polymer-derived voids within the silica shell.

Here we report using $(NH_4)_2SO_4$ to fabricate well-defined hollow spheres with highly ordered mesostructured silica shells and high void ratios by an aerosol EISA process. As a demonstration of using these particles as delivery vehicles, we loaded them with L-methionine, one of eight essential amino acids, which cannot be produced in the body; L-methionine is essential for the production of creatine, important for proper functioning of muscles and the entire cardiovascular system.[11] It benefits pancreatitis, chronic depression, endometriosis, premature ejaculation, Parkinson's disease, *etc.*[12] L-Methionine is selected as a model drug to demonstrate low-temperature drug encapsulation and release from the hollow delivery vehicles.

Mesostructured silica particles were synthesized by EISA[4] using CTAB as a template to form ordered ~2 nm nanopores and two different ammonium salts as templates of a second population of larger nanopores. Fig. 1 shows representative TEM images of calcined particles formed using CTAB and NH_4Cl or $(NH_4)_2SO_4$ templates.

For the $(NH_4)_2SO_4$ template, each particle has only one spherical void (Fig. S2, ESI†). The shell consists of ordered mesoporous silica. The addition of the salt does not affect greatly the self-assembly and order of the mesostructured shell. The XRD pattern in Fig. S1 (ESI†) shows highly ordered 2D hexagonal mesoporous silica. The nitrogen isotherm of the silica particles, shown in Fig. 2, is type IV typical for mesoporous materials, but with additional adsorption at high P/P_0 and a large hysteresis loop due to the emptying of the large internal cavity at $P/P_0 = 0.5$. For comparison the N_2

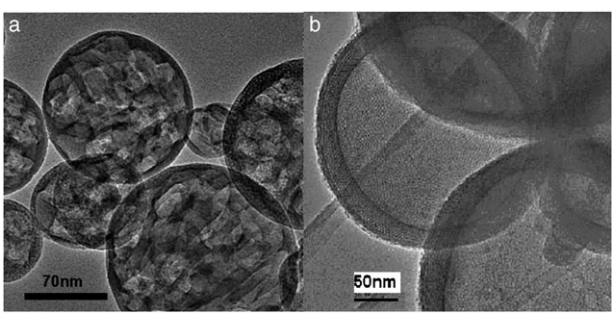

Fig. 1 TEM images for calcined silica particles templated by CTAB and NH_4Cl (a) or $(NH_4)_2SO_4$ (b).

[a] *Department of Chemical and Nuclear Engineering and Center for Micro-Engineered Materials, The University of New Mexico, Albuquerque, NM 87131, USA*
[b] *Aerosol and Respiratory Dosimetry Program, Lovelace Respiratory Research Institute, Albuquerque, NM 87108, USA*
[c] *Department of Chemistry, University of Waterloo, Waterloo, Ontario, Canada N2L 3G1*
[d] *Department of Molecular Genetics and Microbiology, University of New Mexico, NM 87131, USA*
[e] *Sandia National Laboratories, MS 1349, Albuquerque, NM 87106, USA. E-mail: cjbrink@sandia.gov; Fax: +1-505-272-7336; Tel: +1-505-272-7627*

† Electronic supplementary information (ESI) available: Experimental details, aerosol generation, XRD, TEM, and TGA/DTA characterizations, encapsulation and release of L-methionine, and cavity size control by precursor composition. See DOI: 10.1039/b927025f

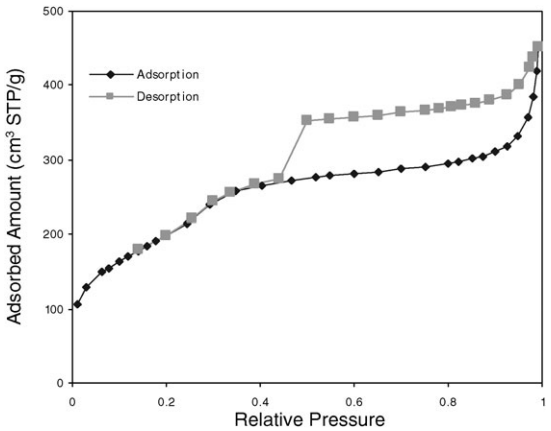

Fig. 2 Nitrogen sorption isotherms of calcined silica sample. Inset is BJH pore size distribution calculated from adsorption isotherm.

sorption isotherm of solid CTAB templated particles formed by aerosol EISA[4] is shown in Fig. S3 (ESI†). The pore width is estimated by the method[13] to be 3.26 nm for the inflection point at $P/P_0 = 0.26$. The pore volume is as high as 0.98 cc g^{-1}, and the fraction porosity is 0.67. The BET surface area is 736 m^2 g^{-1}. The volume ratio for the void measured for the particles is as high as 55%, which is much larger than 31% estimated assuming the void to be templated from a solid ammonium salt core. Such a hierarchical silica structure provides a high volume internal reservoir connected to the particle exterior by a uniform mesoporous shell, promising for high drug loading and controlled drug release.

We further investigated the formation mechanism of the architecture. Solvent evaporation enriches the droplets in surfactant and drives the self-assembly and gelation of the silica mesophase from the droplet surface radially inward.[10] Similar to the case with the NaCl@silica core shell structure,[5] the evaporation of ethanol and water plays a critical role in the formation of the core, shell, and final hollow structures. Simulation of evaporating multi-component droplets indicates that, near the droplet surface, compositional gradients are steeper than the temperature gradient especially for more volatile species due to higher thermal diffusivity than mass diffusivity.[10] $(NH_4)_2SO_4$ is more water soluble than NaCl or NH_4Cl and insoluble in alcohol. Higher water solubility favors later nucleation and formation of fewer and bigger stable $(NH_4)_2SO_4$ nuclei at the droplet center instead of near the droplet surface. As we have demonstrated in numerical simulations[10] for evaporation of ethanol–water–NaCl droplets, the antisolvent, ethanol, favors the formation of a single crystal at the droplet center instead of multiple crystals in the final silica particles. Even though the salt concentration is the highest at the droplet surface, the depletion of the more volatile antisolvent, ethanol, increases the ammonium salt solubility at the droplet surface, making it possible that the first stable $(NH_4)_2SO_4$ nucleus is formed at the droplet center instead of near the surface. Once crystallization starts, quick $(NH_4)_2SO_4$ diffusion quenches the formation of new stable nuclei near the growing nucleus. This favors a single salt core for the small droplet. Additionally, $(NH_4)_2SO_4$ decomposes easily at a temperature of 235 °C, lower than the aerosol heating temperature (400 °C). The ammonia-rich vapor phase formed by decomposition of $(NH_4)_2SO_4$ coalesces into a single large bubble enveloping the salt core to minimize surface energy. It also serves to further promote the condensation of the silica-surfactant phase. As pressure increases, a nearly spherical cavity forms which sustains the silica hollow structure from collapse as the silica condensation reactions eventually solidify and "freeze" the particle structure. Calcination at 500 °C was used to remove CTAB and any remaining $(NH_4)_2SO_4$ to generate the final hollow particles shown in Fig. 1b. The void size can be adjusted by the relative amount of the added ammonium salt and the heating history. Higher heating temperature and longer residence time in the aerosol reactor will enlarge the voids and even cause bursting if too high a temperature is employed. The pore size can be adjusted over a wide range by the surfactant templates. Hollow silica with dense shells can be fabricated if no surfactant is added.

As a comparison, when NH_4Cl was added, multiple voids were dispersed in the final calcined particles as shown in Fig. 1a. NH_4Cl is slightly soluble in ethanol and has lower water solubility than $(NH_4)_2SO_4$, favoring early salt crystallization and formation of multiple crystals. The particle temperature may not exceed the decomposition temperature of NH_4Cl (338 °C), considering the short aerosol reactor residence time (~2 s) and latent heat of solvent evaporation.

The mesopores for $(NH_4)_2SO_4$ templated silica particles are open and permeable to L-methionine. L-Methionine was encapsulated in the hollow structure by repeated heating and cooling of a solution of L-methionine and hollow particles. Upon cooling, L-methionine precipitates on the glass wall of the flask and particle surfaces. During heating surface L-methionine is selectively dissolved by convective transport, while L-methionine inside the voids diffuses slowly due to the transport resistance of the mesostructured silica wall. Upon successive heating and cooling less L-methionine was observed on the flask wall, indicating continued deposition of L-methionine preferentially within the particle void and gradual depletion of drug concentration in the solution. After the drug loading steps, based on TGA/DTA analysis (Fig. S5, ESI†) the weight loss due to L-methionine thermal oxidation is calculated to be 56.3%, nearly the theoretical value (56.6%), assuming complete filling of the voids and mesopores for the hollow particles (pore volume: 0.98 cc g^{-1}). The L-methionine loading is as high as 1.29 g per gram hollow silica. Finally we characterized the release profile for the drug capsules in 1-butanol. The release profile is shown in Fig. S7, ESI.† L-Methionine was released after ~50 min. More rapid nearly burst release is observed in phosphate buffered saline (Fig. S9, ESI†).

In summary, macroscopic phase separation driven by controlled salt nucleation combined with surfactant-templating within aerosol droplets and calcination produces hollow mesoporous silica particles in simple process. Salt decomposition creates a spherical void in the particle center and catalyzes silica condensation stabilizing the hollow particle. This general method can be extended to other metal oxides by optimizing the precursor compositions and aerosol conditions. This aerosol fabrication strategy provides a simple, easy, and

scalable way for fabricating metal oxide hollow spheres with uniform, tunable pore diameters and high surface areas and pore volumes of general interest for drug encapsulation and delivery. The large compartment enables high drug loading. The ability to control pore size and surface chemistry *via* aerosol EISA should enable controlled drug characteristics. Arbitrary drugs can be encapsulated by this approach.

We acknowledge funding from the USA NIH through the NIH Roadmap for Medical Research, DOE Office of Science, Division of Material Science and Engineering and Air Force Office of Scientific Research.

Notes and references

1 J. Panyam and V. Labhasetwar, *Adv. Drug Delivery Rev.*, 2003, **55**, 329–347; K. Uekama, *Chem. Pharm. Bull.*, 2004, **52**, 900–915; S. Freiberg and X. Zhu, *Int. J. Pharm.*, 2004, **282**, 1–18.

2 L. Naldini, U. Blomer, P. Gallay, D. Ory, R. Mulligan, F. H. Gage, I. M. Verma and D. Trono, *Science*, 1996, **272**, 263–267; J. P. Richard, K. Melikov, E. Vives, C. Ramos, B. Verbeure, M. J. Gait, L. V. Chernomordik and B. Lebleu, *J. Biol. Chem.*, 2003, **278**, 585–590; I. I. Slowing, B. G. Trewyn and V. S. Y. Lin, *J. Am. Chem. Soc.*, 2007, **129**, 8845–8849.

3 J. Liu, A. Stace-Naughton and C. J. Brinker, *Chem. Commun.*, 2009, 5100–5102; S. Radin, P. Ducheyne, T. Kamplain and B. H. Tan, *J. Biomed. Mater. Res.*, 2001, **57**, 313–320; S. W. Song, K. Hidajat and S. Kawi, *Langmuir*, 2005, **21**, 9568–9575; J. Andersson, J. Rosenholm, S. Areva and M. Linden, *Chem. Mater.*, 2004, **16**, 4160–4167; J. Liu, A. Stace-Naughton, X. M. Jiang and C. J. Brinker, *J. Am. Chem. Soc.*, 2009, **131**, 1354–1355; J. Lu, M. Liong, J. I. Zink and F. Tamanoi, *Small*, 2007, **3**, 1341–1346; I. I. Slowing, B. G. Trewyn and V. S. Y Lin, *J. Am. Chem. Soc.*, 2007, **129**, 8845–8849; J. Liu, X. M. Jiang, C. Ashley and C. J. Brinker, *J. Am. Chem. Soc.*, 2009, **131**, 7567–7569.

4 Y. Lu, H. Fan, A. Stump, T. Ward, T. Rieker and C. J. Brinker, *Nature*, 1999, **398**, 223–226; M. Bore, S. Rathod, T. Ward and A. Datye, *Langmuir*, 2003, **19**, 256–264.

5 X. M. Jiang and C. J. Brinker, *J. Am. Chem. Soc.*, 2006, **128**, 4512–4513.

6 X. L. Yu, S. J. Ding, Z. K. Meng, J. G. Liu, X. Z. Qu, Y. F. Lu and Z. Z. Yang, *Colloid Polym. Sci.*, 2008, **286**, 1361–1368.

7 S. B. Rathod and T. L. Ward, *J. Mater. Chem.*, 2007, **17**, 2329–2335.

8 J. F. Chen, H. M. Ding, J. X. Wang and L. Shao, *Biomaterials*, 2004, **25**, 723–727; Z. Z. Li, L. X. Wen, L. Shao and J. F. Chen, *J. Controlled Release*, 2004, **98**, 245–254.

9 F. Caruso, *Chem.–Eur. J.*, 2000, **6**, 413–419; Y. S. Chung, J. S. Lim, S. B. Park and K. Okuyama, *J. Chem. Eng. Jpn.*, 2004, **37**, 1099–1104; H. Y. Fan, F. van Swol, Y. F. Lu and C. J. Brinker, *J. Non-Cryst. Solids*, 2001, **285**, 71–78.

10 X. M. Jiang, Dissertation, The University of New Mexico, 2006; C. J. Homer, X. M. Jiang, T. L. Ward, C. J. Brinker and J. P. Reid, *Phys. Chem.Chem. Phys.*, 2009, **11**, 7780–7791.

11 http://en.wikipedia.org/wiki/Methionine.

12 http://www.trulyhuge.com/l-methionine-benefits.html.

13 M. Kruk and M. Jaroniec, *Chem. Mater.*, 2001, **13**, 3169–3183.